Chiral asymmetry of anti-symmetric coordinates studied by the Raman differential bond polarizability of *S*-phenylethylamine*

Shen Hong-Xia(沈红霞)[a)†], Wu Guo-Zhen(吴国祯)[a)‡], and Wang Pei-Jie(王培杰)[b)]

[a)] *State Key Laboratory of Low-Dimensional Quantum Physics, Department of Physics, Tsinghua University, Beijing* 100084, *China*

[b)] *The Beijing Key Laboratory for Nano-Photonics and Nano-Structure, Department of Physics, Capital Normal University, Beijing* 100048, *China*

(Received 24 January 2012; revised manuscript received 15 August 2012)

The Raman optical activity (ROA) study on *S*-phenylethylamine is presented by the intensity analyses via bond polarizability and differential bond polarizability. Ample information concerning the physical picture of this chiral system is obtained, and its ROA mechanism is constructed. Especially, we propose that the asymmetric modes and/or the off-diagonal elements of the electronic polarizability tensor are the potential keys to the exploration of ROA.

Keywords: Raman optical activity, intensity study, asymmetric modes, differential bond polarizability, *S*-phenylethylamine

PACS: 33.20.Fb, 33.55.+b，33.70.–w **DOI:** 10.1088/1674-1056/21/12/123301

1. Introduction

The intramolecular current is expected since molecular vibration will cause charges to flow, i.e., electric current, which in turn will induce the magnetic moment. For chiral molecules under right/left circularly polarized light scatterings, the information concerning the coupling of the magnetic moment and also the electric quadrupole moment due to the unevenly distributed charges in the molecule with the vibrationally induced electric dipole is embedded in their respective differential Raman intensities. This is the so-called Raman optical activity (ROA).[1−5] Therefore, ROA offers us a novel spectroscopic tool for exploring the details of this coupling mechanism which is beyond the capabilities of conventional infrared or Raman techniques. In essence, the ROA process is the same as Raman scattering, except that the differential Raman intensities by the right/left circularly polarized light scatterings are stressed. Bearing this in mind for studying ROA, we need to explore the spectroscopic information first from its intensity. During the Raman scattering, the charges in the molecule are excited or disturbed (for the non-resonance case) and are modulated by the vibration, the so-called vibronic coupling. The effect of the excited/disturbed charges on the vibrationally induced electric dipole, magnetic and quadupole moments needs to be considered in ROA. This information is undoubtedly embedded in the scattered light intensity. Therefore, from the spectroscopic viewpoint, analyses of the Raman and ROA intensities are crucial and necessary routes for retrieving the ROA information. This is our philosophy for the ROA study.[6,7] In the past decades, we have developed an algorithm for the study of the Raman intensity.[8] In the present work, first, we will briefly introduce this algorithm. Second, we will demonstrate how this algorithm can be conveniently extended to the study of the differential Raman intensities in ROA. Third, *S*-phenylethylamine will be introduced by using this approach to reveal its chiral properties as far as ROA mechanism (and of course, Raman mechanism) is concerned. Finally, a concluding remark will be drawn and this approach will be evaluated by comparison with the commercially available software for studying ROA.

*Project supported by the National Natural Science Foundation of China (Grant No. 21153001).

†Visiting scholar from the College of Biology and Chemical Engineering, Jiaxing University, Jiaxing 314001, China

‡Corresponding author. E-mail: wgz-dmp@tsinghua.edu.cn

© 2012 Chinese Physical Society and IOP Publishing Ltd

2. Algorithm to derive the bond polarizability

The algorithm for deriving the bond polarizability from the Raman intensity was proposed by Tian *et al.*[8] It has been applied to several cases[9−11] and has revealed significant properties of the Raman excited virtual states. The Raman intensity is related to $\partial\boldsymbol{\alpha}/\partial\boldsymbol{Q}_j$, which shows the response of the electronic charge to the nuclear motion. Here, $\boldsymbol{\alpha}$ is the molecular electronic polarizability, which is a measure of how loosely the charges are bound to the nuclei and $\boldsymbol{Q}_j$ is the nuclear normal coordinate. $\boldsymbol{\alpha}$ is also proportional to the quantity of charges. For retrieving the bond electronic information in the Raman process, we need to derive $\partial\boldsymbol{\alpha}/\partial\boldsymbol{S}_k$ for the bond coordinate $\boldsymbol{S}_k$ from $\partial\boldsymbol{\alpha}/\partial\boldsymbol{Q}_j$ if possible. For brevity, $\partial\boldsymbol{\alpha}/\partial\boldsymbol{S}_k$ will be called the bond (stretch/bend) polarizability. It is noted that the bond polarizability is an indication of the disturbed charge density in the Raman process.

From the proposition by Chantry,[12] Raman intensity $\boldsymbol{I}_j$ of the j-th normal mode with wavenumber ν_j is related to $\partial\boldsymbol{\alpha}/\partial\boldsymbol{Q}_j$ through the formula

$$\boldsymbol{I}_j \sim \boldsymbol{I}_0 \frac{(\boldsymbol{v}_0 - \boldsymbol{v}_j)^4}{\boldsymbol{v}_j} (\partial\boldsymbol{\alpha}/\partial\boldsymbol{Q}_j)^2.$$

Here, I_0 is the intensity of the exciting laser with wavenumber v_0. In fact, the treatment in the wavenumber domain can be extended to the temporal domain[13] if we perform Fourier transform of $I_j(\nu)$ in the wavenumber domain to the temporal domain. Thus, we have

$$\pm\sqrt{\boldsymbol{I}_j} \sim \sqrt{\boldsymbol{I}_0} \frac{(\boldsymbol{v}_0 - \boldsymbol{v}_j)^2}{\sqrt{\boldsymbol{v}_j}} \sum \boldsymbol{L}_{kj} (\partial\boldsymbol{\alpha}/\partial\boldsymbol{S}_k)$$

by transforming Q_j to the bond coordinates S_k through

$$S_k = \sum L_{kj} Q_j,$$

which can be obtained from the normal mode analysis.[14] Then by defining

$$a_{jk} = \frac{(v_0 - v_j)^2}{\sqrt{v_j}} L_{kj},$$

we have the following matrix equation, if only relative intensities and bond polarizabilities are concerned

$$\begin{pmatrix} \boldsymbol{P}_1\sqrt{\boldsymbol{I}_1} \\ \boldsymbol{P}_2\sqrt{\boldsymbol{I}_2} \\ \cdots \\ \cdots \\ \cdots \\ \boldsymbol{P}_{3N-6}\sqrt{\boldsymbol{I}_{3N-6}} \end{pmatrix} = [\boldsymbol{a}_{jk}] \cdot \begin{pmatrix} \partial\boldsymbol{\alpha}/\partial\boldsymbol{S}_1 \\ \partial\boldsymbol{\alpha}/\partial\boldsymbol{S}_2 \\ \cdots \\ \cdots \\ \cdots \\ \partial\boldsymbol{\alpha}/\partial\boldsymbol{S}_{3N-6} \end{pmatrix}.$$

Here, the phase $\boldsymbol{P}_j$ is + or − which cannot be obtained from the experiment and needs to be determined. In this formalism, only the relative magnitudes of the Raman intensities will be of concern. So are the relative bond polarizabilities.

The bond polarizabilities can be figured out if the above matrix equation is inverted and if the phases preceding the intensities can be determined. For the phase determination, various sets of $\{\boldsymbol{P}_j\}$ are tried to obtain $\partial\boldsymbol{\alpha}/\partial\boldsymbol{S}_k$'s which are then checked with physical considerations to rule out the inadequate $\{\boldsymbol{P}_j\}$ sets. Often the matrix equation can be reduced to accommodate only those mainly of stretching coordinates. This is because the bond stretch polarizabilities are usually larger than those of the bending coordinates and often the coupling between the stretching and bending coordinates is small.

Note: the reason why we have this phase problem is simply that since $I_j \approx [\sum L_{kj}(\partial\alpha/\partial S_k)]^2$, from the intensity, we can determine only $|\sum L_{kj}\,(\partial\alpha/\partial S_k)|$ (the absolute value) but not its sign (phase). Hence, we cannot simply determine $(\partial\alpha/\partial S_k)$ without knowing the phases from the intensities. This is quite analogous to the X-ray structural determination in which one not only measures the diffracted spot intensities, but also needs to nail down their phases in order to solve the structure.

3. Algorithm to derive the differential bond polarizability

For the ROA experiment, we have $I_j^{\mathrm{R}} + I_j^{\mathrm{L}} = I_j$ and $I_j^{\mathrm{R}} - I_j^{\mathrm{L}} = \Delta I_j$ (R and L denote respectively, the right and left circularly polarized scatterings), i.e.,

$$I_j^{\mathrm{R}} = (I_j + \Delta I_j)/2 \quad \text{and} \quad I_j^{\mathrm{L}} = (I_j - \Delta I_j)/2.$$

Hence, we have

$$\begin{bmatrix} \partial\Delta\alpha/\partial S_1 \\ \partial\Delta\alpha/\partial S_2 \\ \vdots \\ \partial\Delta\alpha/\partial S_t \end{bmatrix} = \begin{bmatrix} \\ a_{jk} \\ \\ \end{bmatrix}^{-1} \begin{bmatrix} P_1(\sqrt{I_1^{\mathrm{R}}} - \sqrt{I_1^{\mathrm{L}}}) \\ P_2(\sqrt{I_2^{\mathrm{R}}} - \sqrt{I_2^{\mathrm{L}}}) \\ \vdots \\ P_t(\sqrt{I_t^{\mathrm{R}}} - \sqrt{I_t^{\mathrm{L}}}) \end{bmatrix}.$$

Here, $\Delta\alpha$ is defined formally as $\alpha^{\mathrm{R}} - \alpha^{\mathrm{L}}$ by $\partial\alpha^{\mathrm{R}}/\partial S_k - \partial\alpha^{\mathrm{L}}/\partial S_k$ which is related to the intensities by the right and left circularly polarized scatterings. Consider

$$\begin{aligned} \sqrt{2I_j^{\mathrm{R}}} &= \sqrt{I_j + \Delta I_j} = \sqrt{I_j}\left[\sqrt{(1 + \Delta I_j/I_j)}\right] \\ &\approx \sqrt{I_j}[1 + \Delta I_j/2I_j], \\ \sqrt{2I_j^{\mathrm{L}}} &= \sqrt{I_j - \Delta I_j} = \sqrt{I_j}\left[\sqrt{(1 - \Delta I_j/I_j)}\right] \\ &\approx \sqrt{I_j}[1 - \Delta I_j/2I_j] \end{aligned}$$

with error $< [\Delta I_j/I_j]^2/8$, then

$$\sqrt{I_j^{\mathrm{R}}} - \sqrt{I_j^{\mathrm{L}}} \approx \Delta I_j/\sqrt{I_j}$$

and

$$\begin{bmatrix} \partial\Delta\alpha/\partial S_1 \\ \partial\Delta\alpha/\partial S_2 \\ \vdots \\ \partial\Delta\alpha/\partial S_t \end{bmatrix} = \begin{bmatrix} \\ a_{jk} \\ \\ \end{bmatrix}^{-1} \begin{bmatrix} P_1(\Delta I_1/\sqrt{I_1}) \\ P_2(\Delta I_2/\sqrt{I_2}) \\ \vdots \\ P_t(\Delta I_t/\sqrt{I_t}) \end{bmatrix}.$$

Though I_j is much larger than ΔI_j by an order of 10^3 to 10^4, the relative magnitudes (note this is what we will be concerned with) of I_j's and ΔI_j's can be treated independently as not too small numbers. Hence, $\Delta I_j/\sqrt{I_j}$ can be also treated as not too small numbers.

Once the bond polarizabilities are obtained from I_j's together with the elucidated P_j's and ΔI_j's, which are obtained from the ROA experiment, relative $\partial\Delta\alpha/\partial S_k$ can be obtained at hand. $\partial\Delta\alpha/\partial S_k$ can be called differential bond polarizability, for convenience. This molecular parameter is important for our interpretation of the physics behind the ROA spectrum.

4. Experimental and the normal mode analysis

S-phenylethylamine was purchased from the Aldrich Chemical Co. Ltd. and used without further purification. Its Raman spectrum was recorded by using a Renishaw Invia Raman spectrometer. A 50× objective was used to perform backward scattering. The excitation line was 532 nm from a semiconductor laser. The laser power on the sample was about 10.0 mW. The entrance slit width was 50 μm and the integration time was 20 s. For our purpose, only the relative intensities were considered. In the case where there was spectral profile overlap, de-convolution software was used to resolve the profile into Lorentzian components. Also, the background was offset in measuring the Raman intensity if necessary. The ROA spectrum was measured by using a Biotool chiral RAMAN ROA spectrometer excited by a 532-nm laser with a focused power of 400 mW.

The structure of *S*-phenylethylamine was optimized through DFT B3LYP with 6-31+ basis. The molecular structure and its atomic numberings are shown in Fig. 1. The measured Raman and ROA spectra are shown in Figs. 2 and 3. Together with the normal mode analysis, the mode assignments can be made. The mode frequencies, their Raman and ROA mode intensities, and potential energy distributions (PED) are given in Table 1 (only those that are related to the following analysis are presented). Since the ROA spectrometer can only cover the spectral range below 1800 cm^{-1}, corresponding to the stretching and bending motions of the molecular skeleton of *S*-phenlyethylamine, and the coupling of its skeletal motion with the C–H and N–H moieties is rather weak, we will pay our attention only to this spectral range. We also note that the couplings of C7–H15, N9–H_2 stretching motions with those of the phenyl C–H and C8–H_3 stretchings (around 3000 cm^{-1}) are very weak. Hence, from the Raman intensities due to the C7–H15 and N9–H_2 stretching modes (also listed in Table 1), their bond polarizabilities can be readily obtained.

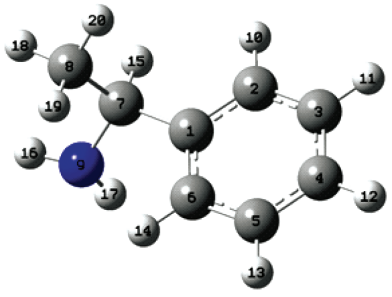


Fig. 1. (color online) *S*-phenylethylamine structure and its atomic numberings. The numbers 1 to 8 refer to the carbon atom, number 9 refers to the nitrogen atom, and the rest represent the hydrogen atom.

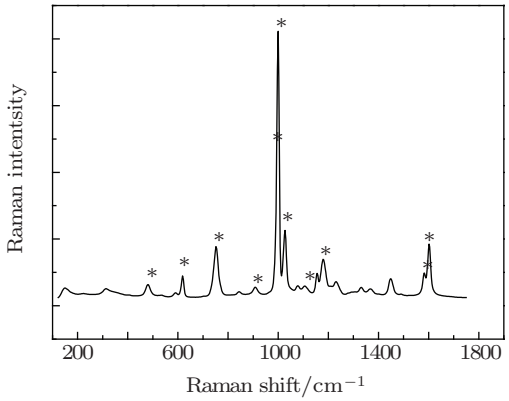


Fig. 2. Raman spectrum of *S*-phenylethylamine. Those marked with ∗ are employed for intensity analysis. See text for details.

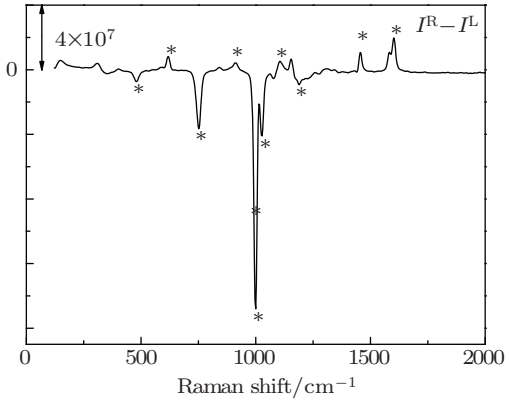


Fig. 3. The ROA spectrum of *S*-phenylethylamine. Those that are marked with ∗ are employed for intensity analysis. See text for details.

Table 1. For *S*-phenylethylamine, the mode wavenumbers, the Raman and ROA intensities, and potential energy distributions (only those that have the values larger than 10 are shown). ∗ by calculation, *r* for bond stretching. See text for details.

Experimental wavenumber	Raman intensity	ROA intensity	Potential energy distribution
3372.0	11.4	–	$r_{\mathrm{NH2\ asym\ str}}(100)$
3314.0	63.5	–	$r_{\mathrm{NH2\ sym\ str}}(108)$
2716.9	6.6	–	$r_{\mathrm{C7H15}}(100)$
1604.5	21.2	+15.1	$r_{\mathrm{C1C2}} + r_{\mathrm{C1C6}}(18)$, $r_{\mathrm{C2C3}} + r_{\mathrm{C5C6}}(52)$, $r_{\mathrm{C3C4}} + r_{\mathrm{C4C5}}(12)$, ring asym def(12)
1584.4	6.9	+5.6	$r_{\mathrm{C1C2}} - r_{\mathrm{C1C6}}(32)$, $r_{\mathrm{C3C4}} - r_{\mathrm{C4C5}}(39)$, C4H12 rocking(11), ring asym def (11)
1376.0*	0.0	0.0	$r_{\mathrm{C2C3}} - r_{\mathrm{C5C6}}(32)$, $r_{\mathrm{C3C4}} - r_{\mathrm{C4C5}}(22)$, ring CHrocking (21), ring CHrocking (22), C7C8NH15 asym def(10)
1349.0*	0.0	0.0	$r_{\mathrm{C1C2}} - r_{\mathrm{C1C6}}(38)$, $r_{\mathrm{C2C3}} - r_{\mathrm{C5C6}}(13)$, $r_{\mathrm{C3C4}} - r_{\mathrm{C4C5}}(18)$, C7C8NH15 asym def(11)
1182.0	27.8	–2.6	$r_{\mathrm{C1C7}}(15)$, C7C8NH15 asym def(12), NH_2rocking(17)
1109.0	3.5	+7.2	$r_{\mathrm{C7N}}(38)$, C7C8H_3rocking(21)
1029.0	21.8	–21.4	$r_{\mathrm{C3C4}} + r_{\mathrm{C4C5}}(37)$, ring trigonal def(26)
1001.0	100.0	–100.0	$r_{\mathrm{C2C3}} + r_{\mathrm{C5C6}}(14)$, $r_{\mathrm{C3C4}} + r_{\mathrm{C4C5}}(22)$, ring trigonal def(37),
991.4	2.9	0.0	$r_{\mathrm{C7C8}}(20)$,$r_{\mathrm{C7N}}(23)$, C7C8H_3rocking(27), NH_2rocking(15)
911.3	5.0	+5.6	$r_{\mathrm{C7C8}}(43)$, r_{C7N} (20), C7C8H_3rocking(12)
754.0	48.3	–36.8	$r_{\mathrm{C1C2}} + r_{\mathrm{C1C6}}(15)$,$r_{\mathrm{C1C7}}(22)$, ring asym def (24)
621.0	7.1	+5.5	ring asym def (20), C1C7NH15 rocking(11), NH_2wagging(46)
483.4	11.4	–8.2	ring asym def (15), C7C8NH15 asym def(36)

5. Elucidation of bond polarizabilities and differential bond polarizabilities

We choose 9 bond stretching coordinates (corresponding to the skeletal bonds) and 4 bending coordinates to elucidate their bond polarizabilities. The Raman and ROA intensities associated with these coordinates are generally intense and are shown in Figs. 2 and 3 with ∗ sign except two modes with extremely weak intensities as given in Table 1. The 13 locally symmetric coordinates are shown in Table 2 for reference.

Table 2. Coordinates r denotes bond stretching.

Locally symmetric coordinate	In terms of internal coordinates
$S1$	$(r_{C1C2}+r_{C1C6})/\sqrt{2}$
$S2$	$(r_{C1C2}-r_{C1C6})/\sqrt{2}$
$S3$	$(r_{C2C3}+r_{C5C6})/\sqrt{2}$
$S4$	$(r_{C2C3}-r_{C5C6})/\sqrt{2}$
$S5$	$(r_{C3C4}+r_{C4C5})/\sqrt{2}$
$S6$	$(r_{C3C4}-r_{C4C5})/\sqrt{2}$
$S12$	r_{C1C7}
$S13$	r_{C7C8}
$S14$	r_{C7N9}
$S28$	ring asym def
$S40$	C7C8NH15 asym def
$S43$	C1C7NH15 rocking
$S51$	NH_2 wagging

What needs to be mentioned is that the bond polarizabilities of the phenyl C–C stretching coordinates can be elucidated through the polarizabilities of their symmetric and anti-symmetric coordinates (See Table 2). If the phenyl ring possesses strick symmetries such as the D_{6h} group, then the modes with anti-symmetric coordinates will be Raman-inactive. In such a case, all the bond polarizabilities of the six phenyl C–C coordinates are the same. In *S*-phenylethylamine, this symmetry is broken, and the Raman peaks due to the anti-symmetric coordinates show up. Just for convenience, this symmetry breaking can be considered as a pertutbation, then the mode intensities due to the symmetric coordinates will possess more diagonal elements of the electronic polarizability tensor while those due to the anti-symmetric coordinates possess more off-diagonal elements of the electronic polarizability tensor. The merit that we will gain as both symmetric and anti-symmetric coordinates are adopted is that the differential bond polarizabilities of both symmetric and anti-symmetric coordinates can be obtained and that their difference demonstrates their differentiability of the chiral asymmetry. Here, we mean, specifically, the asymmetry that shows chiral effect such as ROA. This is what we expect. We know in general that in the Raman process, the diagonal elements of the electronic polarizability are larger than the off-diagonal elements. We will see later in our analysis that in ROA, on the contrary, chiral asymmetry is more expressed by the anti-symmetric coordinates or the off-diagonal elements of the electronic polarizability.

The conditions for solving the phases are that all the bond stretching polarizabilities are positive, the deviations among the six phenyl C–C stretching polarizabilities are not two-fold (this value is not so crucial) larger than their average and that the polarizability of the phenyl ring deformation ($S28$) is less than that of the phenyl C–C stretching. Then, we have seven phase sets left, in which three phase sets possess too large deviation (over 10 fold) among the six phenyl C–C stretching polarizabilities and one phase set for which the temporal behaviour of the bond polarizabilities is not reasonable with too severe variations. Then, only three phase sets remain. The bond polarizabilities corresponding to these three phase sets are shown in Fig. 4, and therein, for comparison, the bond orders by EHMO for the electronic ground state are also shown. Once the phase set is determined, the differential bond polarizabilities can be obtained readily as demonstrated before. They are shown in Fig. 5.

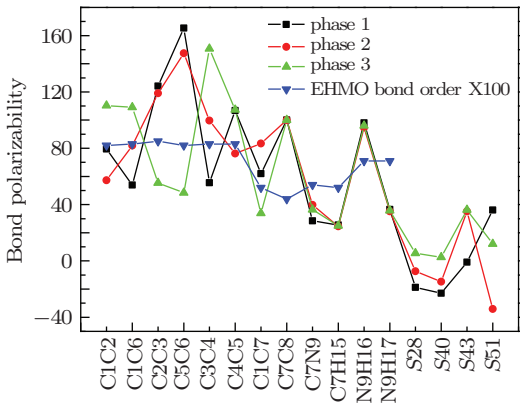


Fig. 4. (color online) Bond polarizabilities, where the polarizability of C7C8 is normalized to 100 for convenience. For comparison, EHMO bond orders of the ground state are also shown. See text for details.

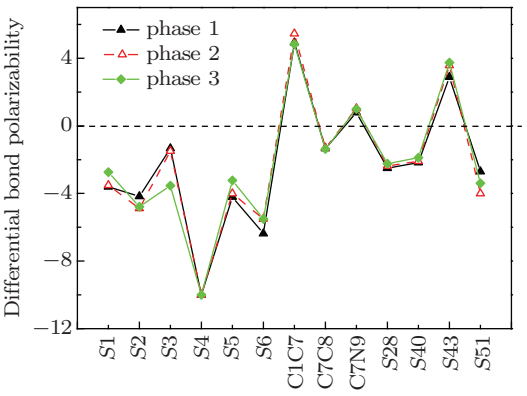


Fig. 5. (color online) Differential bond polarizabilities under various phase sets, where the differential bond polarizability of $S4$ is normalized to -10 for convenience. Note their consistency. See text for details.

6. Physical interpretations of the ROA process

The bond polarizabilities by all the three phase sets demonstrate that in the Raman process, the excited charges are mostly concentrated on C7–C8 and C1–C7 bonds as evidenced by the bond polarizabilities, especially, on the C7–C8 bond which instead possesses the least charges in the ground state by EHMO calculation. The bond polarizability of N9–H16 (N9–H17) is 0.69 of the average of those of the phenyl C–C bonds while EHMO shows this value is 0.86. Evidently, in the excited virtual state, the quantity of charges on the N9–H16 (N9–H17) bond becomes less. For the C7–H15 bond, its polarizability is 0.26 of the average of those of the phenyl C–C bond while EHMO shows that it is 0.63. Evidently, in the excited virtual state, the quantity of charges on the C7–H15 bond is not enhanced significantly, either.

From the elucidated phase sets and the Raman and ROA intensities, the differential bond polarizabilities are readily obtained. Interestingly, these three phase sets lead to consistent differential bond polarizabilities, thus ensuring that the physical interpretations or pictures drawn (from the ROA spectrum) for this chiral molecule are conclusive. From Fig. 5, we have the following observations.

(i) The anti-symmetric $S2$, $S4$, $S6$ coordinates possess the larger polarizabilities than their corresponding symmetric coordinates $S1$, $S3$, and $S5$ coordinates, respectively. In other words, the anti-symmetric coordinates possess stronger ROA or chiral effect. This means that off-diagonal terms of the electronic polarizability tensor show better chiral asymmetry. Specifically, for ROA, we have

$$\Delta\alpha_{xx}, \Delta\alpha_{yy}, \Delta\alpha_{zz} < \Delta\alpha_{xy}, \Delta\alpha_{xz}, \Delta\alpha_{yz},$$

while for the Raman process,

$$\alpha_{xx}, \alpha_{yy}, \alpha_{zz} > \alpha_{xy}, \alpha_{xz}, \alpha_{yz}.$$

This is not difficult to comprehend. Suppose that $\otimes$ is the operation associated with the ROA chiral process. Then, it is expected that $\otimes$ is commutative for the diagonal terms of the polarizability tensor, say (symbolically), $x\otimes x = x\otimes x$ while for the off-diagonal elements, it can be noncommutative, say, $x\otimes y \neq y\otimes x$, leading to $\Delta\alpha_{xy} \neq 0$. Thus, $\Delta\alpha_{xy} > \Delta\alpha_{xx}$, $\Delta\alpha_{yy}$. It is expected that the differential bond polarizability of the anti-symmetric coordinate is larger than that of its counterpart, i.e., the symmetric coordinate which is a general property.

(ii) $S4$, $S6$, and C1–C7 possess the larger differential bond polarizabilities, or stronger ROA effect. As mentioned previously, during the Raman excitation, the excited charges are more concentrated on the C7–C8 bond, playing a role of electric dipole in the ROA electro–magnetic coupling mechanism. The significant differential bond polarizabilities of $S4$ and $S6$ show that the magnetic component in the coupling mechanism comes from the phenyl moiety (though we do not have the ROA spectrum for the phenyl C–H, C7–H15, and N–H_2). This can be related to the charge richness in the phenyl ring (the flow of charges caused by vibration induces the magnetic moment). We note that the differential bond polarizability of $S51$ due to NH_2 wagging is larger than that of $S28$ (phenyl ring asymmetric deformation) and that of $S43$ (C1C7NH15 rocking) is also prominent. All these show that around the asymmetric centre C7, the chiral effect due to the bending motion is more evident than the C7–C8 and C7–N9 stretching. The small differential bond polarizabilities of C7–C8 and C7–N9 can be due to their small magnetic moments since they are farther away from the phenyl ring though the electric dipole on C7–C8 is significant.

7. Concluding remarks

The advent of experimental/spectroscopic techniques in recent decades provides us with quite convenient tools in recording spectra, at least, under certain conditions. The core of spectroscopy remains more on the interpretation and re-construction of the physical/chemical pictures from the spectra. Without doubt, the spectral intensity analysis is a central point, though conventionally, much attention is paid to the frequency domain. As demonstrated in this ROA study on S-phenylethylamine, through the intensity analyses via bond polarizability and differential bond polarizability, ample information concerning the physical picture of this chiral system and its ROA mechanism can be obtained. Especially, we conclude that asymmetric modes and/or the off-diagonal elements of the electronic polariability tensor bear better chiral asymmetries and are the potential keys to the ROA study. Together with the cases of methyloxirane and alanine[7] we studied previously, we confirm that this approach is beneficial and deserves its merits.

Nowadays, people may rely more on handy software such as Gaussian and PyVib2[15−17] for the ROA analysis. It is noticeable that the output parameters by these softwares are mostly mode-dependent such that the bond amplitudes ($\boldsymbol{L}_{kj}$) are not distinguished from these parameters. As demonstrated in our work, our algorithm offers parameters that are mode-independent and they are indeed more deeply rooted molecular parameters. The elucidated physical picture for ROA by our approach will not be apparent if one just looks into the mode-dependent parameters. In this sense, our approach deserves its merits.

References

[1] Barron L D 1982 *Molecular Light Scattering and Optical Activity* (Cambridge: Cambridge University Press)

[2] Barron L D and Buckingham A D 1971 *Mol. Phys.* **20** 1111

[3] Buckinghem A D 1994 *Faraday Discuss.* **99** 1

[4] Nafie L A and Che D 1994 *Adv. Chem. Phys.* **85** 105

[5] Barron L D, Hecht L, Bell A F and Wilson G 1996 *Appl. Spectrosc.* **50** 619

[6] Wang P, Fang Y and Wu G 2011 *J. Raman Spectrosc.* **42** 186

[7] Fang Y, Wu G and Wang P 2012 *Chem. Phys.* **393** 140

[8] Tian B, Wu G and Liu G 1987 *J. Chem. Phys.* **87** 7300

[9] Fang C, Liu Z and Wu G 2008 *J. Mol. Struct.* **885** 168

[10] Liu Z and Wu G 2005 *Chem. Phys.* **316** 25

[11] Wang H and Wu G 2006 *Chem. Phys. Letts.* **421** 460

[12] Chantry G W (Anderson A ed.) 1971 *Polarizability Theory of the Raman Effect in The Raman Effect* Vo1. 1 (New York: Marcel Dekker)

[13] Fang C and Wu G 2008 *Spectrochim. Acta* **71** 1588

[14] Wilson E B Jr, Decius J C and Cross P C 1955 *Molecular Vibrations* (New York: McGraw-Hill)

[15] Hug W 2001 *Chem. Phys.* **264** 53

[16] Zerara M 2008 *J. Comput. Chem.* **29** 306

[17] Hug W and Fedorovsky M 2008 *Theor. Chem. Acc.* **119** 113